SIGNAL: A Ka-band Digital Beam-Forming SAR System Concept to Monitor Topography Variations of Ice Caps and Glaciers

Paco López-Dekker, Marwan Younis, Thomas Börner, and Gerhard Krieger

German Aerospace Center (DLR), 82234 Oberpfaffenhofen, Germany

Email: Francisco.Dekker@dlr.de

INTRODUCTION

This paper describes a novel InSAR mission concept to monitor topographic changes associated with mass change or other dynamic effects on glaciers, ice caps and polar ice sheets. This mission concept, named SIGNAL (SAR for Ice, Glacier aNd globAL Dynamics), was developed, prepared and proposed as an Earth Explorer Opportunity Mission (EE-8). The focus of this paper is on the SAR system concept and the predicted SAR performance, and on the resulting interferometric performance.

The paper starts providing an overview of the mission, including a comparison of the science requirements with the expected mission performance. Then the SAR system design and performance are discussed. Finally, the resulting interferometric performance is discussed.

Mission Overview

SIGNAL is an innovative Ka-band SAR mission concept with the main objective to estimate accurately and repeatedly topography and topographic changes associated with mass change or other dynamic effects on glaciers, ice caps and polar ice sheets. Elevation measurements are complemented with glacier velocity measurements [1], providing valuable additional information for a better understanding of the hydrology of glacierized basins and of the Arc-tic and Antarctic water cycle.

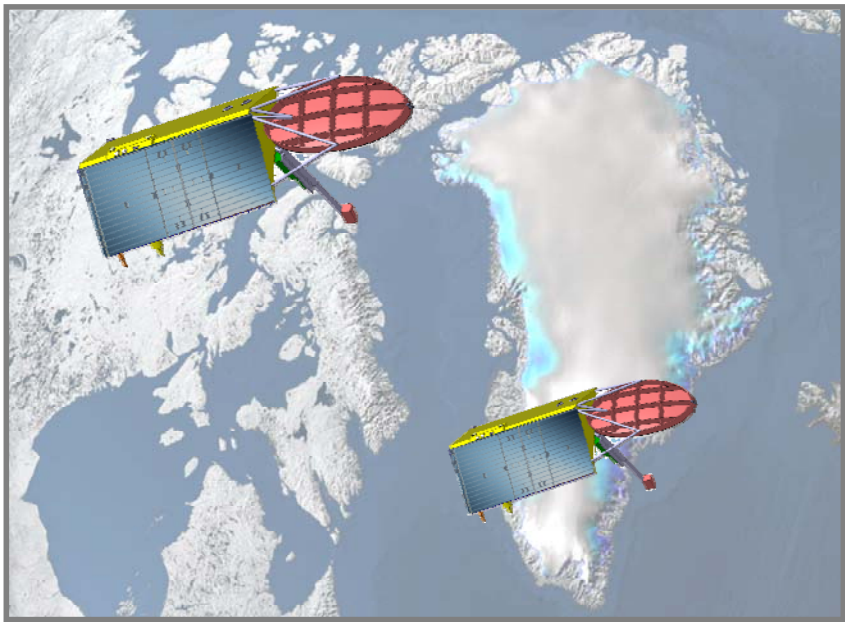

Figure 1 Artist's view of the SIGNAL mission.

The main goal of SIGNAL is to fill major gaps in the data base on mass balance and dynamics of global glacier ice and to thus advance in the knowledge of the processes governing the response of the ice masses to climate forcing. The mission addresses those components of the ice budget that have been subject to accelerated downwasting during the last decade and for which the knowledge of the present mass balance and temporal trends exhibits large error bars: the mountain glaciers and ice caps, and the outlet glaciers of the boundary zones of the Greenland and Antarctic ice sheets.
The driver for the mission design is the generation of digital elevation models of all relevant areas with height accuracies in the order of a few decimeters. This goal justifies two fundamental choices: the use of Ka-band (35 GHz)

to minimize the penetration into the ice or snow cover, in order to obtain a DEM that is truly representative of the surface; and the use of a pair of formation flying satellites, which is the only way to obtain the long baselines required to achieve the desired height sensitivity and measurement stability, avoiding temporal decorrelation effects. SIGNAL is planned as a systematic mapping mission with full coverage of latitudes above 60° North and below 60° South every two months and with a lifetime of at least 5 years, generating seasonal DEMs of the areas of interest.

SAR System Description

In order to provide the required SAR performance in terms of data sensitivity, ambiguity rejection, and coverage, a reflector based system architecture is proposed that uses SCan-On-REceive (SCORE) in order to obtain a sufficiently wide swath despite the narrow, high-gain, receive beam. The total coverage is further increased by simultaneously acquiring two sub-swathes separated by a gap approximately twice the width of a single sub-swath (~ 25 km). A comprehensive description of this system approach is provided in the section *SAR Configuration and Performance*.

Interferometric Performance

In order to meet the science and user requirements, SIGNAL needs to achieve point-to-point relative height errors in the order of a few decimeters, which is an order of magnitude better that TanDEM-X. The two keys to meeting these highly demanding requirements are the very large number of available looks and large, relative to the wavelength, interferometric baseline.

Height Self-Calibration Concept

Aside from noise-like phase errors, which can be mitigated by averaging independent looks, the overall performance of SIGNAL is limited by low frequency systematic phase offsets and baseline uncertainties. In most InSAR scenarios, systematic errors are dealt with by tying the results to reference ground control points. However, in the Arctic and Antarctic regions there are large areas where only few or no ground control points are available. The innovative self-calibration approach is based on using areas, which are imaged by crossing (ascending and descending) ground tracks (see Figure 2). In this case the baseline errors are uncorrelated and have different characteristics. However, there are also other errors affecting the height measures (e.g. coherence loss, height change due to snowfall between acquisitions, etc.), and therefore a Linear Minimum Mean Square Error (LMMSE) estimator in combination with stochastic models for the error sources is used to separate the systematic errors from the real (desired) height variations. It has been shown that with this approach the residual height error can be reduced to decimeter level in areas without ground control points [2], enabling the mission to deliver products with the desired (relative) height accuracy.

The expected performance of the calibration improves as the distance between far and near range increases. In this context, an attractive compromise solution is to divide the total swath in two disconnected sub-swathes, allowing a significant gap in between.

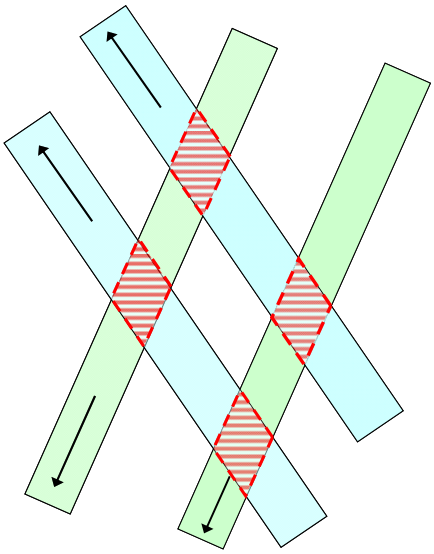

Figure 2 Geometry of ascending (blue) and descending (green) tracks and the corresponding crossings (red) for height calibration w/o ground control points.

Mission performance
Table 1 shows the final performance of SIGNAL, comparing it to the minimum (M) and target (T) science requirements. SIGNAL's end to end performance exceeds in all cases the minimum requirements, and reaches or comes near the target scientific requirements, in particular for the mission-critical ice-dynamics and mass-balance applications.

Table 1. Global interferometric performance. (M – Minimum, T – Target).

Application	Product Resolution (m)	h_{amb} (m)	Predicted Height Error (m)		Sciene Requirement (m)		Notes
			Dry Snow	Wet Snow	M	T	
Ice dynamic	100	14	0.37	0.44	1.0	0.5	DEM difference
Mass balance	200 (100)	14	0.35 (0.37)	0.37 (0.44)	0.5	0.2	DEM difference
Ice sheets DEM	100 (50)	14	0.11 (0.21)	0.27 (0.52)	0.3	0.1	Relative DEM (High Resolution)
	100	14	0.29	0.49	0.3	0.1	Relative DEM (Low Resolution)
Hazards	50	14-20	0.41-0.46	0.63-0.8	2	0.5	DEM difference

SPACE SEGMENT

In the following an overview of the space segment of SIGNAL is given. The main units forming the radar instrument are:

- Parabolic reflector antenna
- Ka-band front-end including Ka-band feed array
- Ka-band transmitter including a Ka-band Extended Interaction Klystrons (EIK),
- Central Radar Electronics consisting of RF Electronics (RFE) and Digital Electronics (DE)
- Synchronization link sub-system

components such as LNAs, circulators, limiters, phase shifter, couplers, isolator, band pass filter, power distribution matrix and Tx phase shifter are not mentioned explicitly.

Antenna Configuration
Large reflector antennas in conjunction with moderate scan rate requirements are simpler and cheaper than array antennas, in particular in Ka-band. In combination with a linear feed array they allow fast scan rates in elevation. The dimensioning of the reflector and feed mainly depends on the required gain and the scan angle range.

The baseline antenna configuration for SIGNAL is a combined Tx/Rx offset parabolic reflector antenna. A high gain antenna is desirable at Ka-band, however the gain of a reflector antenna scales with the reflector size. The maximum reflector size is limited by the envelope of the launcher fairing, which restricts the antenna to parabolic offset reflector of 2.5 m in elevation and 2.5 m in azimuth. Here the antenna length is approximately equal to the required azimuth resolution, which results in a non-optimum instrument operation. The offset antenna configuration is chosen as it has the advantage over a centre fed antenna in that blocking of the antenna aperture by the antenna feed is minimized. This results in a better control of unwanted sidelobes for Tx and Rx and, when transmitting, of unwanted radiation back into the feed.

Ka-Band Transmitter
Ka-band Extended Interaction Kly-strons (EIK) is a possible candidate for the High Power Amplifier (HPA). These already exist based on W-band space qualified models. The published performance figures of EIK for space applications state a peak power of ≈ 3kW at duty cycles in the order of 10% and an efficiency of 40%. These performance figures fulfil most of the requirements.

Baseline is to generate the Ka-band signal level in the RFE and to route the signal via Ka-band waveguide to the EIK. Part of the waveguide is a rotary joint which is necessary because of the deployable feed support structure. The HPA output power is split into multiple identical Tx signals which are routed to the feed horns. Phase shifters between HPA and feed horns are foreseen in order to correct the phase offset of each Tx-branch. A fixed phase offset correction based on on-ground characterisation is sufficient.

Central Electronics
The central electronic performs the analogue-to-digital conversion with bandpass subsampling technique, signal processing, timing generation and instrument control. A chirp generator is used to generate the SAR signal. Because of the low bandwidth (below 50 MHz) the output of the chirp generator is directly modulated on an IF carrier in the order of the third Nyquist frequency. In the receive chain the Ka-band signal of each feed is routed to a low-noise amplifier, combination beam forming network and down-converted to IF.

Front-End
The received radar signals at the output of each feed horn pass the circulators and are routed to dedicated Low Noise Amplifiers (LNA). Couplers between feed array and circulators allow to extract the magnitude and phase of the Tx signal and to use the combined Tx signal for internal calibration. Limiters between circulators and LNAs protect the LNAs against high power levels in Tx mode. The output of the LNAs are routed to the Rx beam switching/formation matrix. This element allows to select on of four Rx beams having fixed pointing angle and beam overlap, respectively. Three feed elements are used for each beam. Dedicated phase shifters located after each LNA are foreseen to correct the phase offset between each feed horn and switching matrix/combiner. The phase shifters allow for a fixed beamforming by adapting the phase offset between the elements. The amplified and combined Rx signal is routed to the RFE via a dedicated deployable waveguide.

Synchronization Link Sub-System
Bistatic operation of the two radar instruments requires phase and time synchronization. Here the same approach as for TanDEM-X is proposed for the synchronization link [13][14][15], which consist of six horn antennas placed on each satellite and used to exchange dedicated synchronization signals between the two satellites. Each satellite transmits and receives synchronization signals. The difference of received sync link signals contains information on relative oscillator drift and oscillator noise. This information is extracted on ground and used to determine (estimate) the correct timing information respectively the relative drift of onboard clock during operation of SAR instruments. By means of proper PRI selection (leap PRI) synchronous operation of both SAR instruments is achieved. In addition the sync link signal is used to estimate and compensate the phase error in interferograms caused by oscillator phase noise.

SAR CONFIGURATION AND PERFORMANCE

The SAR instrument consists of a single reflector used for transmission and reception and a transmit/receive feed array capable of recording multiple channels. The main SAR instrument, orbit, and operation parameters are listed in Table 2. These parameters are used to compute the system performance.

Table 2 Relevant system parameter values for the SIGNAL.

Reflector & Feed		Transmitter		Receiver & Losses	
Parameter	Value	Parameter	Value	Parameter	Value
diameter	2.5 x 2.5 m	av. transmit power	175W	elevation channels	2
focal length	2.5m	duty cycle	10%	two way feed loss	3.7dB
configuration	az. offset	bandwidth	40 MHz	LNA noise figure	2.5 dB
feed elements	22	center frequency	35.75 GHz	atmospheric loss	1.7 dB
antenna tilt angle	32.1°	polarization	linear	polarization	linear
				active Rx elements	2 (of 6)

Orbit/Swath		Operational Mode		sub-swath data		
Parameter	Value	Parameter	Value			
height	740 km	mode	StripMap			
repeat cycle	11 days	sub-swaths	2 (multi)	ssw 1	look angle start/stop	29.90°/31.25°
incidence angle	33.8° – 39.7°	gap	47.9 km		width	25.06 km
look angle	29.9° – 34.9°	polarization mode	HH single			
ground range	434–532km	proc. Doppler bandwidth	2428 Hz	ssw 2	look angle start/stop	33.70°/34.90°
		PRF	6915 Hz		width	24.74 km
		SCORE	yes			

In the following the operation mode of the instrument is detailed, then the SAR instrument performance will be stated.

System Operation

The instrument is operated in the so called multi-diamond SCORE mode. Here SCORE refers to the SCan-On-REceive technique detailed in [1][4][5] adapted to the reflector case in [6][7][8][9]. In a side looking radar system the direction of arrival of the received radar echo is a function of slant range and, therefore, pulse travel time. SCORE in elevation exploits this one-to-one relationship by combining multiple sub-aperture signals such that at each instant of time a narrow beam is steered towards the echo's expected direction of arrival. This enables a high antenna gain without loosing the opportunity for wide swath coverage. A narrow receive beam has the further advantage of attenuating range ambiguities. By combining SCORE technique with a broad transmit beam, a highly sensitive SAR system with wide swath coverage can be built.

On-transmit two different transmit feed configurations are possible:

> **Monostatic or pursuit-monostatic operation**: in this case the single reflector is required to simulta-neously illuminate both sub-swathes, without the in-between gap. The total transmit power is thus distributed on both swathes.
> **Bistatic operation**: Here each satellite can illuminate one of the two sub-swathes with the complete available power. On receive each SAR receives both sub-swathes. In this case the transmit feed net-work is simplified. Compared to the monostatic operation the transmit power can be approximately halved for the same NESZ.

For a reflector fed by a digital feed array, the wide illumination on transmit and SCORE technique on receive can be described as follows: if a single feed element illuminates the complete reflector, a narrow high gain beam is generated which covers typically only a small portion of the swath. In contrast, activation of all feed elements illuminates only a small portion of the reflector resulting in a wide but low gain beam as required for full swath coverage in the transmit mode. On receive, the energy returned from a narrow portion of the ground is collected by the entire reflector and then focused on a small number of feed elements. A radar pulse traversing the swath causes hence the focused energy to sweep through all feed elements within the time period of one pulse repetition interval. When imaging a single swath the receive data stream consists of a summation of the active receive elements and by this does not result in any increased data rate in comparison to conventional SAR.

Several extensions to the basic SCORE mode of operation have recently been proposed [10][11][12]. One of these extensions is to apply multiple receive beams simultaneously, each of which chases an echo while it traverses the ground (c.f. Figure 3 left). By this multi-diamond SCORE (the name originates from the timing diagram, also known as diamond diagram) the swath width can be extended significantly, since it now includes areas, which in a conventional SAR would be regarded as range ambiguities. The multi-diamond SCORE beams are digitally formed using one and the same raw data set, while maintaining the advantages of single-beam SCORE. A particularity of multi-diamond-SCORE are the timing gaps which manifest themselves as blind strips in the SAR image. As seen from the timing diagram in Figure 3 right, the two sub-swathes are separated by a gap approximately double the width of a single sub-swath. The two swathes are imaged simultaneously in a StripMap (not ScanSAR) mode. Note that the timing diagram does not consider the contribution of the nadir returns, since these --in the case of the reflector-- are attenuated by the very low sidelobes of the antenna.

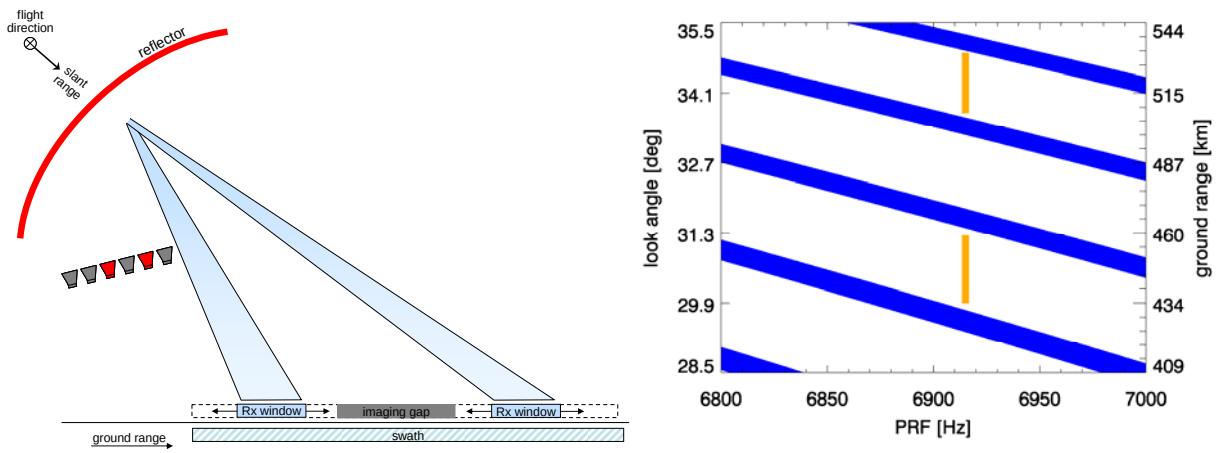

Figure 3. Dual-Diamond operation of SIGNAL instrument where two swathes are imaged simulateneiously in stripmap mode (left: schematic representation, right: timing diagram)

System Performance

Figure 4 shows the ambiguity performance of the system. The processed Doppler bandwidth is 2.4 kHz corresponding to a single look azimuth resolution of 2.5 m. The value of the PRF of ≈ 7 kHz is high compared to the processed Doppler bandwidth which is necessary in order to suppress azimuth ambiguities. This is a design constraint resulting from the small azimuth extend of the reflector, resulting in a wide beam (illuminated Doppler bandwidth) compared to the processed Doppler bandwidth. The resulting azimuth oversampling factor is in the order of 2.8 and is an indication of the amount of on-board data reduction if pre-summing were used.
In range the model basically results in vanishing range ambiguities, which results from the fact that the position of the ambiguities is outside the angular segment covered by the transmit beam and further attenuated by the narrow receive beam.

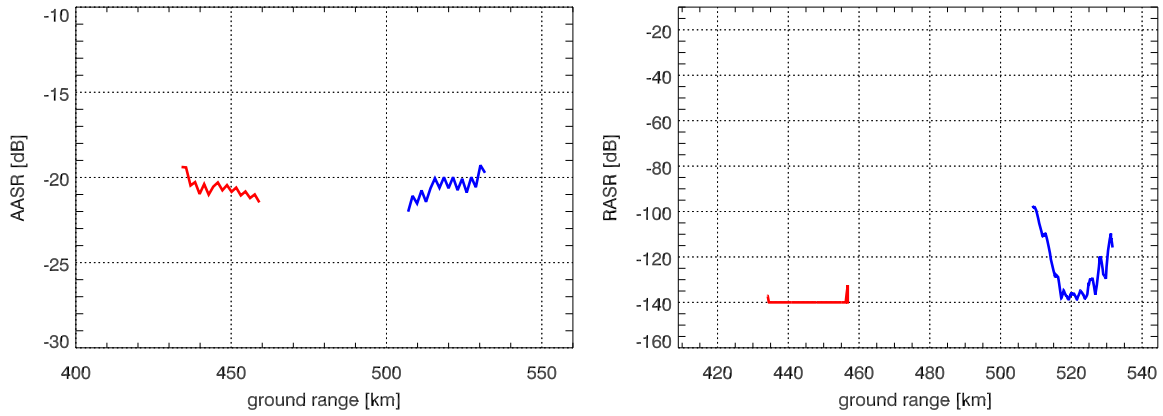

Figure 4. Computed azimuth-ambiguity-to-signal ratio (left) and range-ambiguity-to-signal ratio (right).

The noise performance shown in Figure 5 is computed based on the feed losses and noise figure values given in **Error! Reference source not found.** in addition to an atmospheric loss of 1.7 dB. The average transmit power @ 10% duty cycle is 175 Watt. The pulse extension loss (PEL) is a parameters specific to the SCORE mode of operation which describes the power loss due to the amplitude modulation of the SAR pulse by the (narrow) receive antenna pattern (see [9] for a definition and detailed description). As seen in Figure 5 right the PEL accounts to an additional 0.6 dB of losses which add to the total power budget.

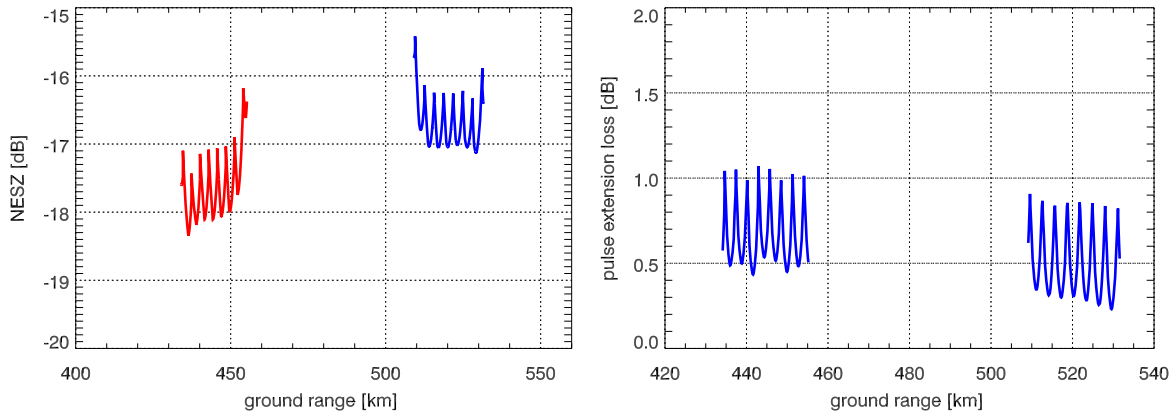

Figure 5. Computed noise-equivalent sigma-zero (left) and pulse extension loss (right).

The resulting data rate taking into account the possible on-board data reduction due to Doppler over-sampling is given in the table below assuming a 10% oversampling in range and azimuth (with pre-summing) and a BAQ 8:3.

Table 3. Data rate for a BAQ 8:3 and 10 % oversampling in range with (azimuth oversampling factor = 2.8) and without azimuth pre-summing.

swath	without pre-summing	with pre-summing
1	200.1 MBit/s	77.5 MBit/s
2	216.6 MBit/s	83.6 MBit/s
total	416.7 MBit/s	161.1 MBit/s

INTERFEROMETRIC PERFORMANCE AND CALIBRATION

Cross-track InSAR (XTI) is a mature and well understood technique, with a well developed theoretical framework that can be applied to predict its performance. This theoretical framework is supported by decades of experimental data. The final height accuracy attainable with an interferometric system depends on

- The geometry of the system.
- Phase degradation due to noise-like decorrelation sources.
- Phase degradation due to instrument errors and geometrical uncertainties (in particular, base-line errors).
- The instrument electrical and mechanical calibration budget.
- Final DEM-level calibration.

Noise-like error sources

Leaving aside systematic errors, the error of the interferometric phase is a zero-mean random variable whose statistics depend on the coherence and the number of looks (i.e. the number of independent samples averaged). For example, the left panel in Fig. 6 shows the 90% confidence value of the phase deviation as a function of the coherence for number of looks ranging from 1 (no averaging) to 4096. This range of looks has been chosen as representative of typical values expected for SIGNAL. Clearly, an increased number of looks rapidly reduces the required coherence to achieve a given quality level.

The interferometric coherence can be written as a function of a number of terms, corresponding to a number of sources of decorrelation

1. Terms that can be safely ignored in single (or near single) pass scenario: temporal decorrelation, clear atmosphere decorrelation and Doppler decorrelation.
2. Geometric decorrelation that is caused by a relative spectral shift of the complex SAR images associated to the interferometric fringes. In the following performance analysis it is assumed that this effect is mitigated by common-band filtering.
3. Volume decorrelation caused by the presence of multiple scattering centers at exactly the same slant-range distance but showing different interferometric phase. Due to the low penetration depth at Ka-band, volume decorrelation resulting from this penetration will be very small. For an infinite layer of an homogeneous medium with a one-way penetration depth given by α (which for snow and Ka-band is around 0.5 m), an analytical expression of the volume decorrelation is given by:

$$|\gamma_{vol}| = \left| \frac{2\alpha/\cos\theta}{2\alpha/\cos\theta + j\Delta k_z} \right|, \text{with } \Delta k_z = \frac{mk_0 B_n}{R\sin\theta} \tag{1}$$

4. Co-registration errors. These depend on how the data are co-registered (e.g. with or without help of an external DEM). For TanDEM-X values around 0.97 are assumed, although it is expected that they can be improved.
5. Decorrelation due to ambiguities. The coherence loss due to ambiguities is estimated as

$$|\gamma_{amb}| = \frac{1}{1+AASR} \cdot \frac{1}{1+RASR} \tag{2}$$

For example, assuming -20 dB azimuth ambiguity to signal ratio (AASR), this gives $\gamma_{amb} \approx 0.99$.

6. Quantization noise. This depends on the assumed quantization scheme and the average number of bits. For 3 bit BAQ quantization, for example, this gives $\gamma_{quant} \approx 0.964$.

7. Decorrelation due to thermal noise. For example, a SNR value of 15 dB, which would correspond to a scenario with a σ_0 of 0 dB, and a NESZ of -15 dB, results in $\gamma_{SNR} \approx 0.97$. The right panel in Fig. 3 shows the 90% confidence normalized point to point relative height error as a function of SNR, again for several numbers of looks and assuming that all non-noise-related decorrelation effects together result in a decorrelation term of 0.9 (solid lines) and 0.96 (dashed lines), respectively. The normalization factor is the height of ambiguity.

In case of homogeneous errors with independent Gaussian distributions, one may approximate the 90% point-to-point height errors by

$$\Delta h^{90\%} \approx 2.33 \cdot \sigma_h \tag{3}$$

where σ_h is the standard deviation of the single-point random height error component. The factor 2.33 is given by the multiplication of $\sqrt{2}$ (accounting for the difference operation between two independent random variables) with a value of 1.65 (accounting for the transition of the standard deviation to 90% errors where the factor 1.65 is easily derived from the Gaussian error function).

For SIGNAL, and depending on the target application, these point-to-point errors may correspond to pairs of points in a single acquisition, or pairs of acquisitions of the same geographical point.

Phase errors are scaled to relative height errors by the height of ambiguity. As an example, Fig. 6 shows the 90% confidence interval height error normalized with respect of the height of ambiguity as a function of SNR for different numbers of looks and assuming that the loss of coherence due to everything that is not noise introduces a decorrelation factor of 0.9 (solid lines) and 0.96 (dashed lines). For example, assuming a coherence given by $0.9 \cdot \gamma_{SNR}$, and a SNR of 10 dB, 512 looks and a 740 km orbit, a normal monostatic baseline of approximately 40 m (or twice as much in a bistatic configuration) is required to achieve the 0.5 meter relative accuracy.

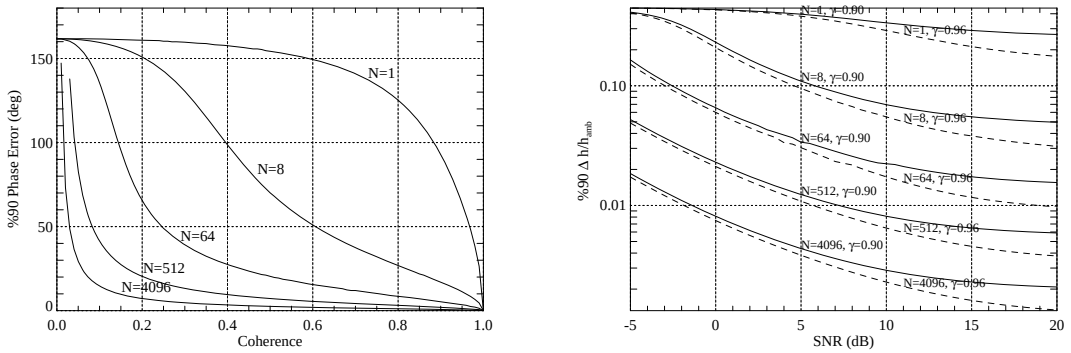

Figure 6 Left: point to point relative phase error (90% confidence interval) vs coherence for different number of looks. Right: Normalized relative height error as function of SNR and number of looks.

Noise like error analysis

In this section, the relative error due to coherence loss is analyzed using the instrument performance model for the dual-swath design discussed in the *SAR Configuration and Performance section*. The phase errors are evaluated under the following assumptions:

- Surface reflectivity is assumed constant, but a range of surfaces is considered. In particular, the results presented in the following sub-sections correspond to scattering coefficients of Alpine dry- and wet- snow, and bare surfaces.
- A constant spectral shift is introduced corresponding to a 20% slope facing the instrument, which is a pessimistic assumption. Perfect common-band filtering is assumed, so that the effect of this spectral shift is a loss of independent samples.
- Volumetric decorrelation is introduced assuming a 1-way penetration depth of 1 meter, which is a conservative assumption.

- Coherence loss due to ambiguities is calculated using (2), with the range dependent range and azimuth ASR given by the performance model.
- The impact of BAQ noise is included using the BAQ performance model derived for the TerraSAR-X mission. The results shown correspond to 8:3 BAQ, which is assumed in order to constrain the data rate.

Fig. 7 shows some 90% relative error examples for dry and wet snow. The top panels show results for a 50 m normal baseline (h_{amb} = 42 - 52 m) and 50 m product ground resolution. The bottom panels correspond to a 150 m normal baseline (h_{amb} = 14 - 17 m) and 200 m resolution. The most salient feature is the gap in the coverage caused by the 50 km separation between the two sub-swathes used in this configuration. The total 100 km span results in a large difference between the near-range and far-range errors, although this variation is similar to the ripple caused due to the NESZ variation inside each swath.

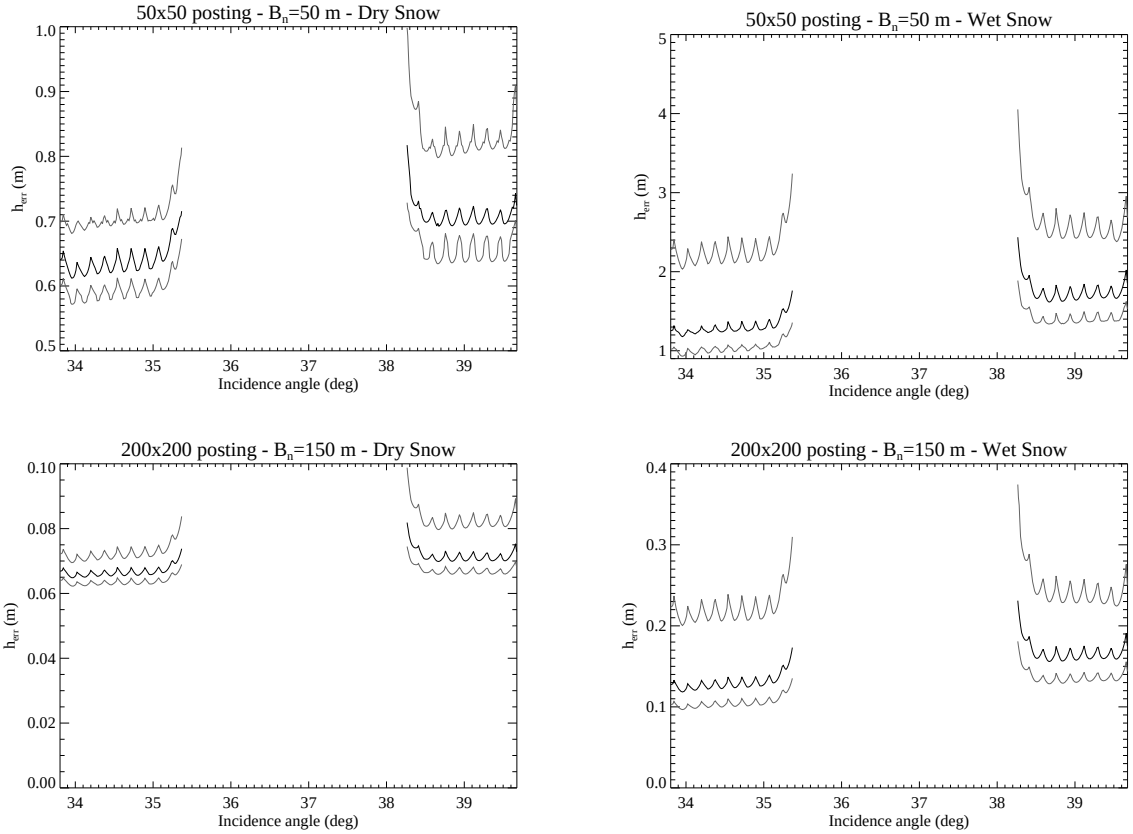

Figure 7 Examples of relative point-to-point height errors for high end (dual-swath) instrument design. All errors represent 90% confidence intervals. The left and right columns correspond to dry and wet snow, respectively. The top panels show results for a 50 m normal baseline (h_{amb} = 42- 52 m) and 50 m product ground resolution. The bottom panels correspond to a 150 m normal baseline (h_{amb} = 14 - 17 m) and 200 m resolution. The 50 km gap between the two sub-swathes is clearly shown.

Acknowledgments

The study was supported by the German Space Agency with funds of the Federal Ministry of Economics and Technology (BMWi) under support code 50 EE 0931.

REFERENCES

[1] M. Villano, A. Moreira, H. Miller, H. Rott, I. Hajnsek, R. Bamler, P. López-Dekker, T. Börner, F. De Zan, G. Krieger, K. Papathanassiou, "SIGNAL: Mission Concept and Performance Assessment," Proc. EUSAR Conference 2010, pp. 520-523, Aachen, Germany, 08.-10. June 2010.

[2] T. Börner, F. De Zan, F. López-Dekker, G. Krieger, I. Hajnsek, K. Papathanassiou, M. Villano, M. Younis, A. Danklmayer, W. Dierking, T. Nagler, H. Rott, S. Lehner, T. Fügen, and A. Moreira, "SIGNAL: SAR for Ice, Glacier and Global Dynamics," Proc. IGARSS Conference 2010, Honolulu, Hawaii, 25.-30. July 2010.

[3] M. Suess and W. Wiesbeck, "Side-looking synthetic aperture radar system," European Patent EP 1241 487, Sept., 2002.

[4] M. Suess, M. Zubler, and R. Zahn, “Performance Investigation on the High Resolution, Wide Swath SAR System,” Proc. European Conference on Synthetic Aperture Radar EUSAR 2002, 2002.

[5] J. H. Blythe, “Radar systems,” United States Patent 4 253 098, Feb. 1981.

[6] M. Ludwig and S. D’Addio, “Ka-Band SAR Feasibility Study,” ESA Document TEC-ETP/2009.122.ML issue 1.0.

[7] G. Krieger, N. Gebert, M. Younis, F. Bordoni, A. Patyuchenko, and A. Moreira, “Advanced concepts for ultra-wide swath SAR imaging,” Proc. European Conference on Synthetic Aperture Radar EUSAR 2008, Friedrichshafen, Germany, June 2008.

[8] J. T. Kare, “Moving receive beam method and apparatus for synthetic aperture radar,” United States Patent 6 175 326, Jan. 2001.

[9] M. Younis, S. Huber, A. Patyuchenko, F. Bordoni, and G. Krieger, “Performance comparison of reflector- and planar-antenna based digital beamforming SAR,” Int. Journal of Antennas and Propagation, vol. 2009, June 2009. [Online]. Available: http://www.hindawi.com/journals/ijap/2009

[10] Krieger, G., Gebert, N., Moreira, A., Multidimensional Waveform Encoding for Spaceborne Synthetic Aperture Radar Remote Sensing, Series Principles of Waveform Diversity and Design, Publisher SciTech Publishing, Inc., Raleigh, NC., pp. 232-256, 2010.

[11] Krieger, G., Gebert, N., Younis, M., Moreira, A., Advanced Synthetic Aperture Radar Based on Digital Beamforming and Waveform Diversity, Proc. RadarCon, Rome, Italy, May 2008

[12] Younis, M., Bordoni, F., Gebert, N., Krieger, G., Smart Multi-Aperture Radar Techniques for Spaceborne Remote Sensing, Proc. IGARSS, Boston, USA, Jul. 2008.

[13] G. Krieger, A. Moreira, H. Fiedler, I. Hajnsek, M. Werner, M. Younis, and M. Zink, “TanDEM-X: A Satellite Formation for High-Resolution SAR Interferometry”, IEEE Trans. on Geoscience and Remote Sensing, vol 45, issue 11, part 1, Nov. 2007, pp. 3317-3341

[14] G. Krieger and M. Younis, “Impact of Oscillator Noise in Bistatic and Multistatic SAR”, IEEE Geoscience and Remote Sensing Letters, Letters, vol. 3, no 3, July 2006, pp. 424-428.

[15] M. Younis, R. Metzig and G. Krieger, “Performance Prediction of a Phase Synchronization Link for Bistatic SAR”, IEEE Geoscience and Remote Sensing Letters, vol. 3, no 3, July 2006, pp. 429-433.